

Signal Acquisition and Processing of the Moving Vehicle Weighing System

SHENGYAO JIA, QING LI, XIONG LI
 College of Electrical and Mechanical Engineering
 China Jiliang University
 China Jiliang University, Hangzhou, 310018
 CHINA
 E-mail:darlbar@126.com

Abstract: - Through experiments we have found that the weight of the lighter axle of the two-axle vehicle would become heavier than its static weight and the heavier axle would become lighter than its static weight when the vehicle speed becomes faster. Based on this conclusion, a novel weighing method for vehicles with middle high speed is set up. It has also reduced the error caused by the impact of vehicle vibrating. System hardware, software and design ideas for vehicle Weigh-In-Motion (WIM) have been introduced in this article. The system also has the advantages of easy installation and portability.

Key-Words: - Weigh-In-Motion , Compensation , Axle-Weight

1 Introduction

With the development of transportation and carrying trade, the number of overloaded vehicles and their speed has got larger and larger. The weighing of in-motion vehicles is becoming very important. Its main purpose is to check for overloaded and ensure the normal life of the road. Compared with the static weighing system, the key features of WIM system are saving time, efficient and causing no disruption to normal traffic. This has extremely important significance for highway construction and management. At the same time, the modern management of vehicle transportation also has a greater role in promoting.

2 System Design

2.1 Signal Acquisition of Axle-weight

The detectors of the weighing system are two composite slab sensor boards which are installed on the road. The weighing system measures each axle-weight of a vehicle while it passes the sensor boards shown in Fig.1.

The total weight of the vehicle could be estimated by the sum of each axle-weight which is the key for us to calculate. Transition board in front of the sensor is to reduce the shock pressure on the sensor

board while vehicle rolling from the ground. Block diagram of the WIM system is shown in Figure 2, including two-way sensors, two amplifiers, an acquisition card and a computer. Pressure signals are converted into analog signals by sensors. After

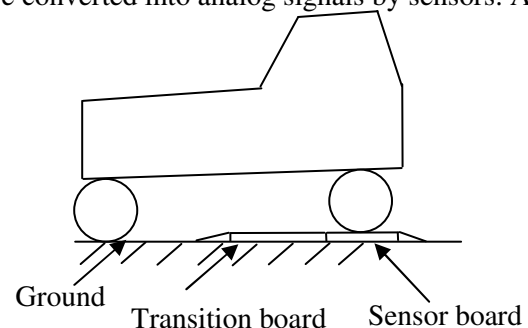


Fig.1.The diagram for WIM experiment

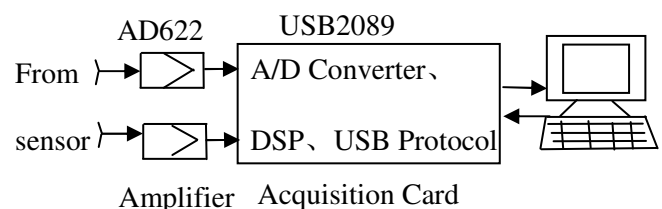


Fig.2. The block diagram of the system

amplified by AD622, analog signals are converted into digital signals through acquisition card. At last,

digital signals are input into a computer. We use the computer for signals processing such as storage, analysis and calculating.

2.2 Hardware Design

As dynamic weighing, the measured pressure signals are very short-lived. We choose Amp AD622 which has fast dynamic response, high sensitivity and linearity. Its signal transmission rate is up to $1.2V/\mu s$. The sampling frequency of acquisition card that we choose is 50 KHz, 25 KHz for each channel. Acquisition card has USB interface, through that the data collected can be transmitted to the computer. These dynamic indicators have been able to meet the performance of the system of signals transmission, gathering requirements.

2.3 Software Design

After installed Acquisition Card Driver on computer, we can set various parameters of the acquisition card such as sampling frequency, sampling channels, sampling ways with driver functions. The procedures of interface part between acquisition card and computer have become very simple. The key points of computer programming are multi-line operations that allow computer dealing with multiple events at the same time.

2.3.1 Necessity for Multi-line Operations

Our equipment is usually working in a single-CPU but multi-tasking environment. As frequently switching between tasks, especially when we move windows, or pop-up dialog boxes, etc, the current thread will suddenly spend a lot of time to deal with these graphics operations. On the other hand, the sampling frequency is very high. If not handled properly, we may not be able to achieve high-speed uninterrupted data collection.

2.3.2 Solution Method

To address this problem we create two sub-threads, one is data collection thread, and the other is data processing thread. Data collection thread is absolute worker thread, only responsible for data collection. At the same time, data processing thread is processing data that from collection thread such as displaying the data in the current window and storing the data in computer. The relationship between these two sub-threads is shown in Figure.3.

First, data collection thread and data processing thread are started at the same time. Then data collection thread begins to collect data and data pro-

-cessing thread keeps into hibernation until synchronization signals have been sent to it. After

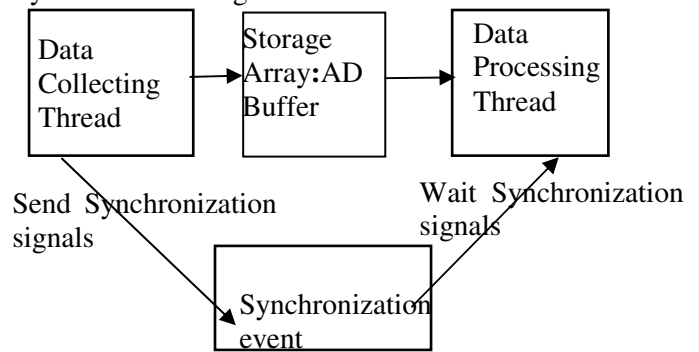


Fig.3.Relationship between sub-threads

8k data collection completed, data collection thread would send synchronization signals to trigger data processing thread and continue to collect data. Data processing thread then begins to data processing which has been storied in array AD Buffer. One cycle is end.

Finally, we create a function for vehicle weight processing and call it following data processing thread.

3 Signal Processing

3.1 Signal Filtering

The voltage signals shown in Figure 4 are collected by one channel of the acquisition card. They are pressure signals of one side of the automobile front and rear axle-weight. Vertical axis is voltage signals, abscissa axis is collection points.

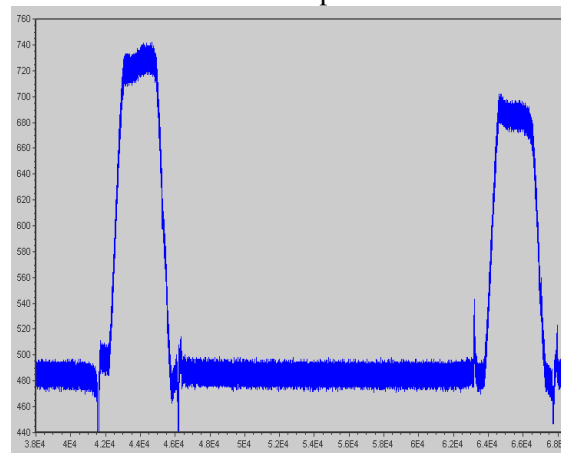


Fig.4.Voltage signals of one side of two-axle vehicle axle-weight.

We can see that pressure signals have been superimposed on a number of noise signals. We use FIR digital low-pass filtering and average filtering algorithm to deal with them in computer.

FIR low-pass filter is primarily seeking the response of finite length units $h(n)$. In the Digital Filter Design of MATLAB software, we have chosen 50 bands low-pass filter with Hamming Window, selected cut-off frequency as 1KHz (too small will cause significant voltage signals attenuation). After that $h(n)$ can be exported from MATLAB. Set $y(n)$ as filtered signal, and $x(n)$ as what need to be filtered, $z(0), z(1), \dots, z(49)$ are all 0, then

$$z(n) = x(n - 50), n \geq 50 \tag{1}$$

$$y(n) = \sum_{m=0}^{50} h(m) * z(50 + n - m) \tag{2}$$

We only need to program-calculate the two formulas in computer. $Y(n)$ is shown in Figure 5.

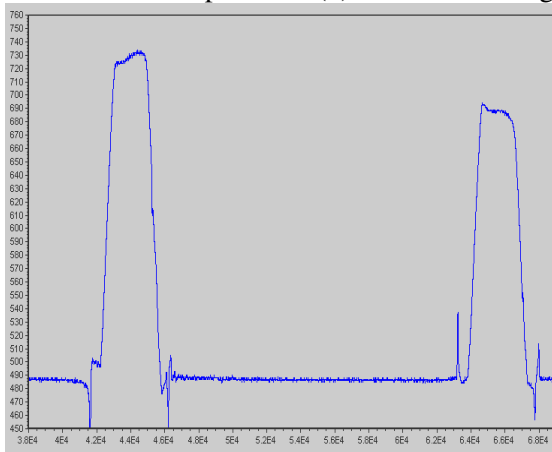


Fig.5. Filtered graph of Fig.4

The advantage of FIR low-pass filter is that the number of data points before filtered and after filtered is equivalent with strictly linear phase. But the disadvantages are also obvious, the calculation of FIR low-pass filter is a large quantity considering the data points we collected for each test often tend to reach hundreds of thousands to millions. Therefore, we have adopted average filtering algorithm.

Average filtering algorithm is simple. We seek a data point from each 25 points on the average. Filtered graph is shown in Fig.6. The disadvantage of average filtering algorithm is that the number of data points after filtered is 1/25 of number before filtered. However, since the sampling frequency is high and the total number of data points is very large, we can get enough valid signals from the filtered points. Average filtering method's advantag-

-es are also significant, simple programming and fast computing speed provide a great convenience for the follow-up calculation.

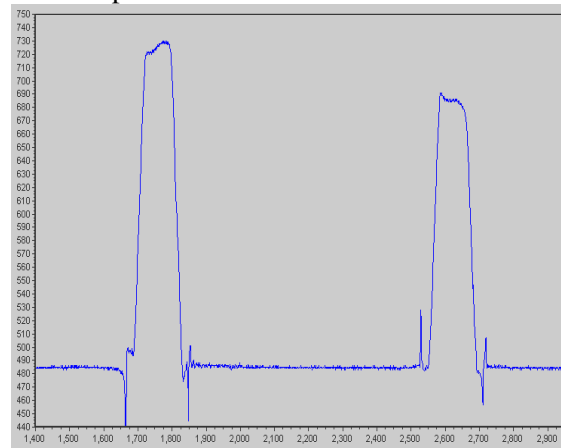


Fig.6. Filtered graph of Fig.4 by average filtering algorithm

3.2 Step Test

3.2.1 Simulate Ideal Step Signal

The purpose of doing step test is to measure the time of sensor response. If response time is not rapid, there is not much sense for dynamic weighing with this kind of sensor boards. However, to simulate an ideal step signal on the sensor is not easy.

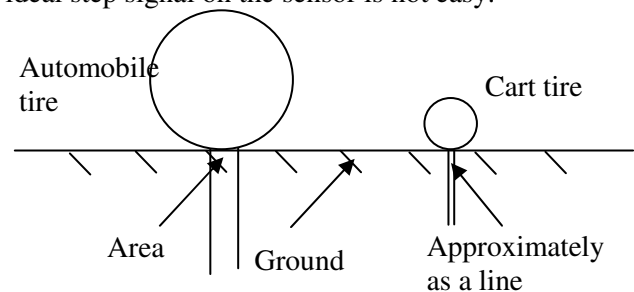


Fig.7. Area that automobile tire and cart tire contacted with ground

First, we drove vehicle slowly and stopped it on the sensor boards to simulate step signals. It was later discovered that in fact were slope signals. Because automobile tire contacted with the ground is not a line but an area in which the weight of vehicle is slowly superimposed on the sensor boards, shown in Figure.7.

Then we use cart for test, which has 5 wheels, two rows of four wheels behind, one wheel in front. The wheels of the cart are made by hard material, deformation degree can be ignored. Since the wheel is very small, the area of the wheel contacted with

the ground can be approximated as a line. We upload 600kg weight in the cart and quickly push

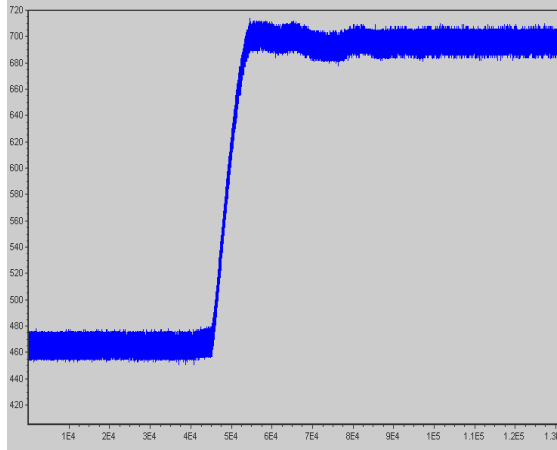


Fig.8. Slope response of the sensor

the front wheel on the sensor board. The whole process can be seen as step signals superimposed on the sensor board. We can see step response in Fig.9.

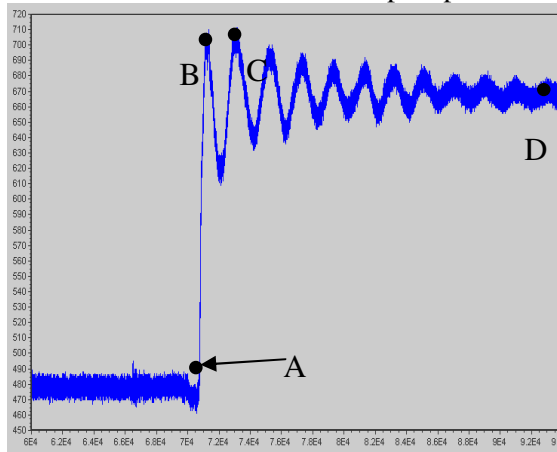


Fig.9. Step response

We consider that the time from point A to point B is the peak time. The wheel is not stopping rolling until point C and system begins to stabilize at point D. When we calculate the performance indicators of step response, the time from point B to point C need to be removed.

3.2.2 Identify the Step Curve

In order to get dynamic parameters such as peak time, overshoot and so on, step curve needs to be recognition. We first use least-square method for identification of this step curve.

For the SISO discrete-time stochastic system, the equation of description is

$$z(k)+a_1z(k-1)+a_2z(k-2)+\dots+a_{n_a}z(k-n_a)=b_1u(k)+b_2u(k-2)\dots+b_{n_b}u(k-n_b)+e(k) \quad (3)$$

$Z(k)$ is the output of step response, $u(k)$ is the static weight of cart axle and $e(k)$ is random noise. Its square format is

$$z(k) = \vec{h}^T(k)\vec{\theta} + e(k) \quad (4)$$

$$\vec{h}^T(k) = [-z(k-1), \dots, -z(k-n_a), u(k-1), \dots, u(k-n_b)]^T,$$

$$\vec{\theta} = [a_1, a_2, \dots, a_{n_a}, b_1, b_2, \dots, b_{n_b}].$$

Take criterion function $J(\vec{\theta})$ as

$$J(\vec{\theta}_{LS}) = \sum_{k=1}^L [e(k)]^2 = \sum_{k=1}^L [z(k) - \vec{h}^T(k)\vec{\theta}]^2 \quad (5)$$

To obtain the minimum value of $J(\vec{\theta}_{LS})$

when $\vec{\theta} = \vec{\theta}_{LS}$, then $\frac{\partial J(\vec{\theta})}{\partial \vec{\theta}} \Big|_{\vec{\theta}=\vec{\theta}_{LS}} = 0$. After transformation we can get

$$\vec{\theta}_{LS} = (\vec{H}_L^T \vec{H}_L)^{-1} \vec{H}_L^T z_L \quad (6)$$

In equation 6, $\vec{\theta}_{LS}$ can be solved through computer programming with fourth-order least-square method. Then we get the equation after identification

$$z1(k) = 1.4484 * z1(k-1) - 0.4142 * z1(k-2) + 0.0402 * z1(k-3) - 0.1224 * z1(k-4) + 0.0940 * u(i-1) + 0.0154 * u(i-2) - 0.0558 * u(i-3) - 0.0048 * u(i-4) \quad (7)$$

In the calculations, input $u(k)$ need to be superimposed on white noise to ensure that $\vec{H}_L^T \vec{H}_L$ is a regular matrix. The amplitude of white noise is ± 1 . Before calculations, $z(k)$ and $u(k)$ need to

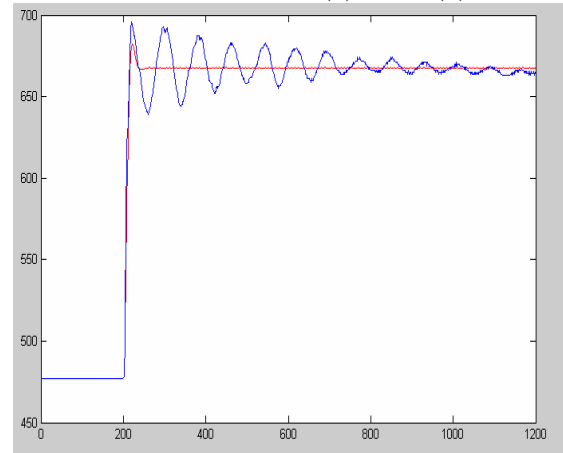


Fig.10. Least-square fitting curve

remove the initial value which is the sensor response of no-load. The red line is the fitting curve $z1(k)$, and the blue line is $z(k)$, shown in Fig.10.

Another way for recognition is the second-order transfer function fitting method. Through peak time and overshoot, we can calculate damping ratio ξ and natural frequency of the system ω_n . With sampling interval 1ms, discrete transfer function is expressed as

$$\frac{Y(z)}{U(z)} = \frac{0.01544z + 0.01454}{z^2 - 1.804z + 0.8342} \quad (8)$$

$$z^2 * Y(z) = (1.804z - 0.8342) * Y(z) + (0.0154z + 0.01454)$$

$$*U(Z) \quad (9)$$

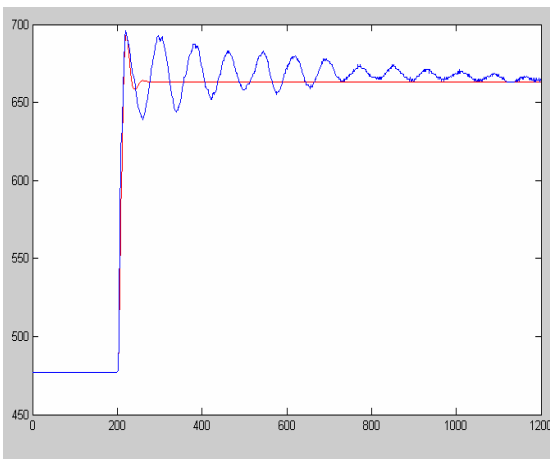


Fig.11. Transfer Function fitting curve

Convert it to differential equation,

$$y(k) = 1.804 * y(k-1) - 0.8342 * y(k-2) + 0.01544 * u(k-1) + 0.01454 * u(k-2) \quad (10)$$

Before calculations, $z(k)$ and $u(k)$ need to remove the initial value and plus it in the final result. The red line is $y(k)$. Fitting curve is shown in Fig.11.

3.2.3 Conclusions from Step Test and Analysis of Measured Waveform

Through identification by these two methods, we can estimate that the peak time of the sensor is 20ms or so. Taking into account the area that cart's wheel contracted with the ground is not a line, the actual peak time is even smaller. Whether the peak time is associated with the weight or not need to do further research. But the axle-weight of the vehicle we used to do experiments is similar with the step test, 20ms is still an important reference value for peak time.

The width of sensor's effective measurement is 0.32m and the speed of vehicle is no more than

30Km/h. In this case, we are fully capable of measuring the effective signals of the axle-weight.

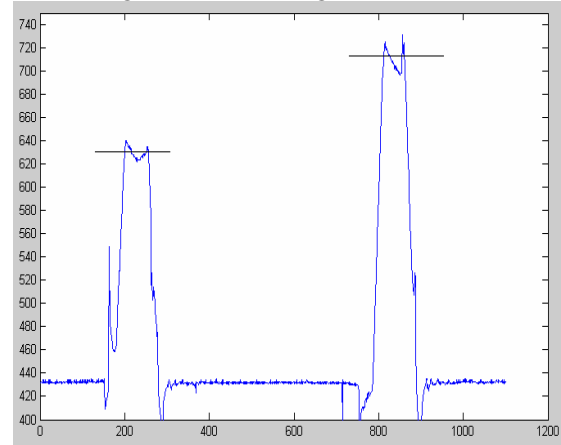


Fig.12. Voltage signals of one side of two-axle vehicle axle-weight, V=16Km/h.

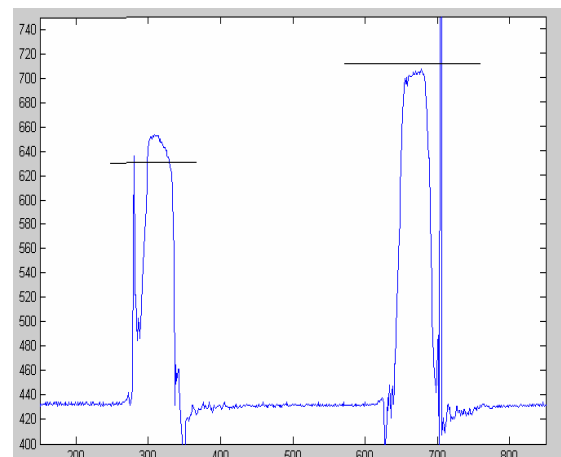


Fig.13. Voltage signals of one side of two-axle vehicle axle-weight, V=33Km/h.

Figure 12 and Figure 13 show the axle-weight signals we have measured by the same vehicle with different velocities. Black line is the static weight of the axle. The crest of the curve is concave in Figure 12 but convex in Figure 13. That means vehicle would be vibration with low vibration frequency when it is moving. From the two figures, we can see that faster the speed, heavier the front axle-weight and lighter the rear axle-weight. Lots of experimental results show that the weight of the lighter axle of the two-axle vehicle becomes heavier than its static weight and the heavier axle becomes lighter than its static weight when the speed becomes faster. What causes this phenomenon and whether it is associated with the type of vehicle or not need to do further research?

3.3 Effective Signals Extraction

In this step, we need to extract axle-weight signals for next step calculations from filtered signals. In Figure 14, axle-weight signals are the peak data points. We average the first 100 data points, and record the result as x .

$$y = x + 55\text{mV} \quad (11)$$

$$y1 = x + 35\text{mV} \quad (12)$$

Then we take y as a starting voltage for axle-weight. The voltage of a point is higher than y and its followed subsequent 15 points are all higher than that, this point is the starting point, recorded as z . Since z , when the voltage of a point is smaller than $y1$ and its followed subsequent 15 points are all smaller than that, this point is the ending point, recorded as $z1$. From this point, automobile's wheels begin to leave the sensor boards.

Data points between z and $z1$ is what we need to calculate for the vehicle axle-weight, shown in Figure 14.

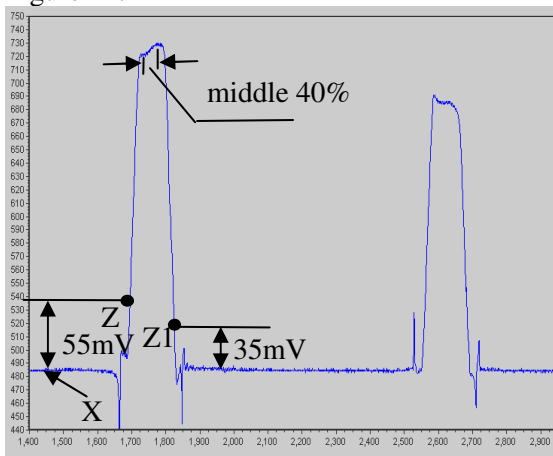


Fig.14.Extract axle-weight signals from filtered signals.

Of course, the selection of these points is based on the need of a certain basis. After calibration tests, 55 mV is corresponding to the weight of about 100Kg. Most of the vehicle axle-weight is much heavier than that. On the other side 55mV can filter out most of noise and interference signals. Axle weight signals extractions have been taken the principle of holding and sustainability. The signals that are higher than the initial signals and also need to maintain a period of time can serve as starting signals. This can avoid the impact of pulse signals when vehicle moving on the sensor boards from the ground. The data points of pulse signals are higher than y , but maintain for a very short time and they are interference signals.

3.4 Axle-Weight Signal Processing

Considering the vibration component caused by motion of vehicle, it is difficult to estimate the weight of vehicle in high accuracy. When the automobile is upward vibration, the result is underestimated. When it is downward vibration, the result may be overestimate. In this paper, we judge the vibration upward or downward according to bump level of the measured waveform, and give appropriate compensation. Currently, signals processing are divided into two grades. One grade is for the weight of the vehicle below 5 tons, the other is for the weight of 5 tons or more. We take the former as an example to discuss axle-weight signals processing.

3.4.1 Select the middle data points according to velocity

When the velocity is less than 13.4Km / h, we select the middle 50% data points between z and $z1$, shown in Fig.14. When it is faster than 13.4Km / h and less than 20Km / h, we select the middle 40%. When it is faster than 20Km / h, we select the middle 30%. Because the faster the velocity the less effective points we measured, the data points we take are closer and closer to the middle.

3.4.2 Calculate the changes of slop

The points we select are divided into two parts. The changes in slop of each part will be calculated. For example, we get 12 points, denoted by Sum (1), Sum (2) ... Sum (12), then

$$Xielv1 = ((Sum1 - Sum4) / 3 + (Sum2 - Sum5) / 3 + (Sum3 - Sum6) / 3) / 3 \quad (13)$$

$$Xielv2 = ((Sum7 - Sum10) / 3 + (Sum8 - Sum11) / 3 + (Sum9 - Sum12) / 3) / 3 \quad (14)$$

3.4.3 Classify the waveform according to Xielv1 and Xielv2

The peak shape of the waveform is determined by the value of Xielv1 and Xielv2. The bound is ± 1 . When Xielv1 or Xielv2 is bigger than 1 or smaller than -1 means the peak of waveform has significantly decreased or increased. According to the bump level, waveform is divided into 3 categories, shown in Figures 15, 16, 17.

Type1; Typical example is shown in Fig.15. $Xielv1 > 1$, $Xielv2 < -1$ and $Xielv1 < -1$, $Xielv2 < -1$ are also fall into this category.

Type2; Typical example is shown in Fig.16. $Xielv1 < -1$, $Xielv2 > 1$ and $-1 < Xielv1 < 1$, $Xielv2 > 1$ are also fall into this category.

Type3; Typical example is shown in Fig. 17, including these points $-1 < Xielv1 < 1$, $-1 < Xielv2 < 1$.

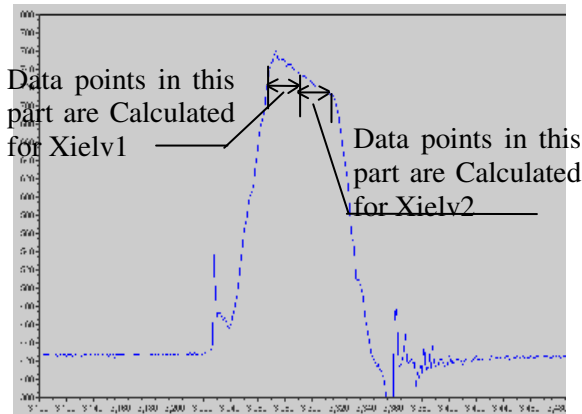


Fig.15. One of the waveforms of $Xielv1 > 1$, $Xielv2 > 1$

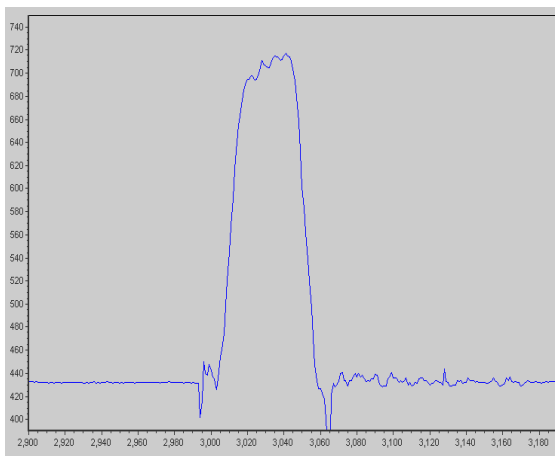


Fig.16. One of the waveforms of $Xielv1 < -1$, $-1 < Xielv2 < 1$

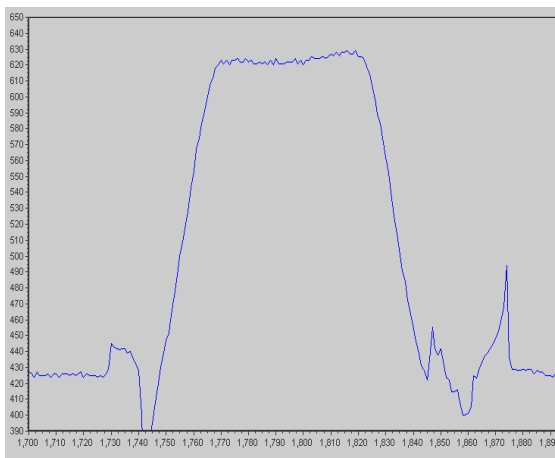


Fig.17. One of the waveforms of $-1 < Xielv1 < 1$, $-1 < Xielv2 < 1$

3.4.4 Compensation according to the type of waveform and vehicle speed

In this step, we compensate the waveform according to waveform type and vehicle speed. Compensation method is the positive half cycle of sine function will be added to the data points we have selected between z and $z1$. We get final axle-weight of the vehicle by averaging the compensated data points. The frequency of sine function is determined by the amount of compensated data points. The amplitude is determined by the waveform type and vehicle speed, it is the value of experience. It has been selected through a large number of dynamic experiments and the static measurements. On the other hand, faster the speed, greater the amplitude of sine function.

Set the number of compensated data points as x , then the frequency of sine function is as follows:

$$f = 1000 / (2 * x) \tag{15}$$

In the equation, sampling interval for each point is 0.001s, 2 means of half a cycle. The compensation equation is shown as follows:

$$g(i) = Co * A * Sin(f * 2 * \pi * i) \tag{16}$$

A is determined by the bump of waveform, set

$$Xielv = |Xielv1| + |Xielv2| \tag{17}$$

$Xielv < 5$, $A = 1$; $5 \leq Xielv < 8$, $A = 2$; When $A > 8$, then

$$A = 1 + Int(Xielv / 4) \tag{18}$$

Int means of rounding function. Co is determined by the waveform type and vehicle speed. Coefficient Co is the biggest in the first type of waveforms, followed by the second type, and the third type is the smallest.

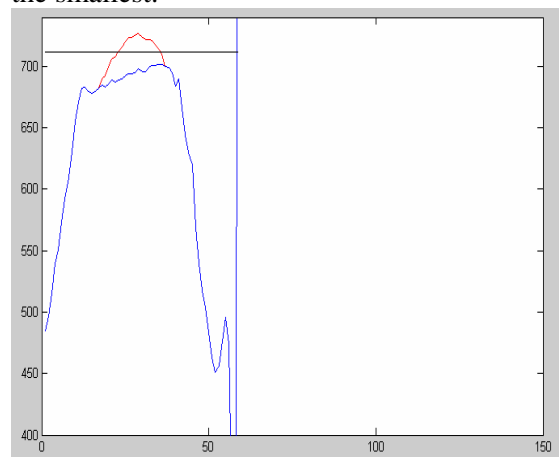


Fig.18. Compensated waveform

In Fig.18, blue curve is the waveform before compensated, belongs to the first category. As speed is 25Km/h, we have selected middle 30% data points for calculating axle-weight and compensation.

By calculating, $X_{i1}v_1=-1.25$, $X_{i2}v_2=-1.125$, $A=1$, $f=24$, then compensation equation

$$g(i) = 30 * \sin(24 * 2 * \pi * i) \quad (19)$$

Red curve is the waveform after compensated and black curve is static weight of axle. After compensated, axle weight is 713mV, compared to 693mV before compensated and 712mV of static signals, we can conclude that error caused by vibrating has been significantly decreased by compensation.

Table1 and Table2 show the results of the axle-weight and total weight of the vehicle which have been real-time displayed in computer when we do experiments.

4 Conclusions

In this paper, we have found that the weight of the lighter axle of the two-axle vehicle would become heavier than its static weight and the heavier axle would become lighter than its static weight when the vehicle-speed becomes faster. Based on this conclusion, a novel weighing method for vehicles with middle high speed is set up. By judging changes of the peak-slop, we classify the waveform of axle-weight into different categories and compensate them which have reduced the error caused by the impact of vehicle vibrating. Currently, the measurement accuracy is less than 10% when the weight of 2-axle vehicle is not more than 20 tons and the velocity is lower than 20Km/h. For the weight of vehicle is not more than 3 tons, measurement accuracy can reach 5% or below when the velocity is lower than 30Km/h. Measurement results can be real-time displayed in measuring site.

However, this method also has its limitations. Waveforms belong to the first category have a good compensation effect, this kind of waveforms are concave. But waveforms belong to the second category are protruding. The results of this kind before compensated may be greater or smaller than the static value. If it was greater before compensated, we would make more and more errors through compensation.

No.	axle of Left front (kg)	axle of Left rear (kg)	axle of right front (kg)	axle of right rear (kg)	velocity (Km/h)	Total weight (kg)	Static weight (kg)	Relative error
1	413	510	350	506	28.29	1779	1758	1.2%
2	376	523	357	531	25.55	1787	1758	1.6%
3	423	508	352	488	28.8	1771	1758	0.7%
4	421	499	357	479	24.37	1756	1758	-0.1%
5	344	482	404	464	26.4	1694	1758	-3.6%
6	394	499	399	466	33	1758	1758	0.0%
7	374	310	367	322	9.16	1373	1388	-1.0%
8	350	287	408	333	29.33	1378	1388	-0.7%
9	406	327	382	314	25.14	1419	1388	2.2%

Table.1.The weight of vehicle is no more than 3 tons.

No.	axle of Left front (kg)	axle of Left rear (kg)	axle of right front (kg)	axle of right rear (kg)	velocity (Km/h)	Total weight (kg)	Static weight (kg)	Relative error
1	3001	2612	2853	2876	15.48	11342	10587	7.1%
2	2649	2594	2713	3174	11.52	11130	12452	10.6%
3	2418	2996	2740	3627	20.87	11781	12452	5.3%
4	2734	3392	2767	4855	16.18	13748	12452	10.4%
5	2624	3447	2735	4326	12.74	13132	14380	8.6%
6	2589	3696	2727	4271	12.52	13283	14380	7.6%
7	2675	4303	2806	5552	11.16	15336	16423	6.6%
8	2672	3982	2734	5584	11.16	14972	16423	8.8%
9	2418	4372	3511	7146	11.71	17447	18332	4.8%
10	2742	5078	3082	6771	12.74	17673	18332	3.6%

Table.2. The weight of vehicle is no more than 20 tons.

References:

- [1] Cebond, Coordinator B J. Weigh-in -motion of axles and vehicles for Europe (WAVE) [R]. General Report, 2001.
- [2] Thissen U., Brakel R.V., et al. Using support vector machines for time series prediction[J]. Chemo metrics and Intelligent Laboratory Systems, 2003,69(1-2):35-49.
- [3] Wang Jinfang, Wu Mingguang. An Overview of Research on Weigh-in-motion System[C].Proceeding of the 5th World Congress on Intelligent Control and Automation, 2004, 6:5241 –5244.
- [4] Cheng Lu, Zhang Hongjian, Xuan Qi. Application of Support Vector Machine to Vehicle Weigh-in-Motion Systems, Proceedings of the Third International Symposium on Instrumentation Science and Technology, 2004.
- [5] Lu Cheng, Hongjian Zhang, Qing Li. Design of a Capacitive Flexible Weighing Sensor for Vehicle WIM System, Sensors, 2007, 7(8):1530-1544.
- [6] Yang, S. Micro-capacitance sensor based on a four-phase detection technique [J].Journal of Transducer Technology, 2003,22:13-15.
- [7] Brian Taylor, Dr. Art Began, et al. The Importance of Commercial Vehicle Weight Enforcement In Safety And Road Asset Management [J]. Traffic Technology International 2000, Annual Review.
- [8] Boleslaw Mazurek, Tomasz Janiczek, et al. Assesment of vehicle weight measurement method using PVDF transducers [J]. Journal of Electrostatics, 2001, 51-52: 76-81.
- [9] Shenfang Yuan, Fahard Ansari, et al. Optic fibber-based dynamic pressure sensor for WIM system [J]. Sensors and Actuators A, 2005, 120: 53-58.
- [10] Gillespie T.D, S.M Karamihas, et al. Effects of Heavy-Vehicle Characteristics on Pavement Response and Performance [R]. NCHRP report 353, National Research Council, Washington, D.C., 1993.
- [11] Michael S. Mamlouk. Effect of Vehicle-pavement Interaction on Weigh-in-Motion Equipment Design [J]. Heavy Vehicle Systems, 1996: 306-322.
- [12] Lombaert G., Degrande G. The experimental validation of a numerical model for the prediction of the vibrations in the free field produced by road traffic. Journal of Sound and Vibration, 2003, 262: 309-331.
- [13] Yang, S. Micro-capacitance sensor based on a four-phase detection technique [J]. Journal of Transducer Technology, 2003, 22: 13-15.
- [14] James G. Stratham. The Oregon Dot Slow-Speed Weigh-in-Motion Project [R]. Oregon Department of Transportation Research Unit, 1998.
- [15] T. Ono. On dynamic weighing of highway vehicles in motion [C]. SICE Annual Conference, 2003,2: 2108 - 2115.
- [16] M. Mangeas, S. Glaser, V. Dolcemascolo. Neural networks estimation of truck static weights by fusing weight-in-motion data [C]. Proceedings of the Fifth International Conference on Information Fusion. 2002,1:456-462.